



# Isolation of a novel quercetin derivative from *Terminalia chebula* and RT-PCR-assisted probing to investigate its DNA repair in hepatoma cells

Kallyadan Soumya, Karickal Raman Haridas, Jesna James, and Sudhakaran Sudheesh\*

School of Chemical Sciences, Kannur University, Payyanur Campus, Edat P.O., Payyanur, Kannur, Kerala, India - 670327

## Abstract

**Background and purpose:** DNA damage can lead to carcinogenesis if replication proceeds without proper repair. This study focused on the purification of a novel quercetin derivative present in *Terminalia chebula* fruit and studied its protective role in hepatoma cells due to H<sub>2</sub>O<sub>2</sub>-DNA damage.

**Experimental approach:** The pure compound obtained from the silica gel column was subjected to structural characterization using spectroscopic techniques. MTT assay was employed to select a non-toxic concentration of the isolated compounds on HepG2 and Chang liver cells. The antigenotoxic property of the compound on HepG2 and Chang liver cells was carried out by alkaline comet assay. Analyses of expression levels of mRNA for two DNA repair enzymes, OGG1 and NEIL1, in HepG2 and Chang liver cells, were carried out using the RT-PCR method.

**Findings/Results:** The pure compound obtained from the fraction-5 of diethyl ether extract was identified as a novel quercetin derivative and named 7-(but-2-en-1-yloxy)-2-(4(but-2-en-1-yloxy)-3-hydroxyphenyl)-3-(hexa-2,4-dien-1-yloxy)-6-hydroxy-4H-chromen-4-one. This compound recorded modest toxicity at the highest concentration tested (percentage cell viability at 100 µg/mL was 64.71 ± 0.38 for HepG2 and 45.32 ± 0.07 for Chang liver cells). The compound has demonstrated noteworthy protection against H<sub>2</sub>O<sub>2</sub>-induced DNA damage in both cell lines. Analyses of mRNA expression levels for enzymes OGG1 and NEIL1 enzymes in HepG2 and Chang liver cells asserted the protective role of the isolated compound against H<sub>2</sub>O<sub>2</sub>-induced DNA damage.

**Conclusion and implication:** The protective effect of a novel quercetin derivative isolated from *T. chebula* in the hepatoma cells is reported here for the first time.

**Keywords:** Antigenotoxicity; Chang liver cell; HepG2 cell; NEIL1, OGG1; Quercetin derivative; *T. chebula*.

## INTRODUCTION

An insight into the formation of reactive oxygen species (ROS) is vital to establishing and improving an effective antioxidant defense system against the toxic oxidants that cause devastating effects within the body. ROS are mainly produced in living organisms as a by-product of normal metabolic processes and are also generated by environmental factors like exposure to electromagnetic radiation, chemical oxidants, chemotherapeutic drugs, etc. (1). Since it is especially stable and freely diffusible, among the ROS, hydrogen peroxide

may cause damage to almost every component of a living cell. Thus, it could reach the nucleus and then intermingle with cellular components like DNA. ROS is a prime cause of a variety of DNA damage, namely oxidation of bases, abasic sites, and single-strand and double-strand breaks. Inefficient remediation of oxidative DNA base damage by DNA repair mechanisms leads to mutation, the initiation and progression of cancer (2).

\*Corresponding author: S. Sudheesh  
Tel: +91-9847421467  
Email: sudheeshs@kannuruniv.ac.in

### Access this article online



Website: <http://rps.mui.ac.ir>

DOI: 10.4103/RPS.RPS\_56\_23

Due to the lower redox potential, guanine is easily susceptible to base lesions. Over 100 types of DNA lesions have been identified, 7,8-dihydro-8-oxoguanine (8-oxoG) is one of the significantly studied and common DNA base lesions created by ROS (3,4). It has been assumed that approximately 180 guanine bases are oxidized to 8-oxoG per cell each day. It acts as a mutagenic miscoding lesion that preferentially mispairs with adenosine and leads to G: C to A: T transversion mutations. Since there exists a strong relationship between ROS generation and 8-oxoG formation, the level of 8-oxoG is often considered a biomarker of oxidative stress (5). After oxidative stress, other lesions like formamidopyrimidine, 2,6-diamino-4-hydroxy-5-formamidopyrimidine (FapyG), and 4,6-diamino-5-formamidopyrimidine (FapyA) are also forged at equal or higher levels than 8-oxoG. These lesions are caused by the hydroxyl radical attack on the bases of guanine and adenine (6).

Oxidative DNA damage is mainly repaired by the base excision repair (BER) pathway. The BER pathway involves several genes; the primary step acts as DNA glycosylases. They remove the N-glycosylase bond between the base and the sugar, thus releasing the damaged base and forming an abasic site called an AP site (apurinic/apyrimidinic site). Several glycosylases recognize more than one type of cleavage. 8-Oxoguanine DNA glycosylase (OGG1) protein was found to exhibit strong specificity for 8-oxoG and FapyG, with no significant specificity for FapyA. While the endonuclease VIII-like 1 (NEIL1) protein efficiently excises FapyG and FapyA, it has not been shown to have specificity for 8-oxoG (1,6).

*Terminalia chebula*, commonly known as black myrobalan and belonging to the Combretaceae family, is a popular folk medicine prevalently cultivated in India and Southeast Asia (7). It has been studied for its homeostatic, antitussive, laxative, diuretic, and cardiogenic activities (8). *T. chebula* is widely used as a traditional medicine to cure several ailments, such as digestive and coronary disorders, coughs, and skin disorders (9). The *T. chebula* fruits are reported to have complex phytochemicals that can be used for managing a variety of diseases like cancer, cardiovascular,

digestive problems, etc. The extracts obtained from this plant are also reported to have significant antibacterial activity against several bacterial species (10). Moreover, it is deemed an effective measure in inhibiting *Helicobacter pylori*, *Xanthomonas campestris*, and *Salmonella typhi*. Furthermore, significant antifungal activity against numerous dermatophytes and yeasts was also reported by the aqueous extract of *T. chebula* fruit (11).

The current study zeroed in on the antigenotoxic activity of a novel flavonoid purified from *T. chebula* on H<sub>2</sub>O<sub>2</sub>-caused DNA damage in the hepatocarcinoma (HepG2) and Chang liver cell lines. Additionally, the effect of the isolated compound on the expression levels of mRNA for the DNA repair enzymes encoding OGG1 and NEIL1 in HepG2 and Chang liver cells was measured employing the real-time polymerase chain reaction (RT-PCR) technique.

## MATERIALS AND METHODS

### *Chemicals and reagents*

The chemicals and solvents used for extraction and purification were of the highest purity and procured from Merck, India.

### *Preparation of T. chebula fruit extracts*

Fresh fruits of *T. chebula* were purchased from the herbal medicine supplier in Kannur district, Kerala, India. The sample was authenticated by Dr. Sujanal P, Scientist, Kerala Forest Research Institute (KFRI), Thrissur, Kerala, India and deposited in KFRI. The collected seeds were initially cleansed with pure water, shade-dried, and ground into a powder form. The soxhlet extraction method was used to prepare 80% of the methanolic extracts. The extracts were washed with petroleum ether to remove fatty matter. The filtrate was then partitioned with diethyl ether and ethyl acetate. Both the ethyl acetate and diethyl ether extracts were dried in a fume hood and thus obtained solid residues were stored in a desiccator.

### *Isolation and purification of flavonoids from T. chebula extracts*

The extracts (diethyl ether and ethyl acetate) obtained from *T. chebula* fruit were subjected

to column chromatography to isolate the active components. A clean and dry glass column was filled with a slurry of silica gel (60-120 mesh size) using hexane. Each extract weighing 15 g was thoroughly mixed with a small amount of silica gel and loaded onto the top of the respective column. Once the sample was loaded, the column was eluted with varying ratios of hexane: ethyl acetate and ethyl acetate: methanol (12). Fractions of 20 mL from each solvent system were collected and further analyzed with thin-layer chromatography (TLC). To isolate the active principles, the fractions with similar  $R_f$  values were combined and concentrated with the aid of a rota vacuum flash evaporator. The entire pooled fractions were investigated for the presence of flavonoids and further subjected to *in vitro* antioxidant activity studies. Fraction 5 was obtained from the diethyl ether extract which yielded a pure compound. This compound recorded significant antioxidant properties and thus was selected for a thorough structural elucidation process.

#### **Structural characterization of the compound**

UV-visible spectroscopy, Fourier transform infrared spectroscopy (FT-IR), proton nuclear magnetic resonance spectroscopy ( $^1\text{H}$  NMR), and mass spectroscopy were used to determine the chemical structure of the isolated compound from fraction 5. From 200 to 600 nm, the UV-visible spectrum was recorded on a Shimadzu UV Pharmaspec-1700 spectrophotometer (Japan) with spectroscopic-grade methanol as the solvent. FT-IR spectrum of the compound was recorded in transmission mode with a Shimadzu FT-IR spectrometer-8400S, in the wave number range of 400-4000  $\text{cm}^{-1}$  using potassium bromide (KBr) pellets. A Bruker Ascend 500 MHz spectrometer (Germany) was used to collect  $^1\text{H}$  NMR spectra with  $\text{CD}_3\text{COCD}_3$  (deuterated acetone) as the solvent and TMS tetramethyl silane as the internal standard. The purified compound's mass spectrum was recorded using a Thermo Fisher Scientific high-resolution mass spectrometer (USA; HR-MS).

#### **Cytotoxicity of the isolated pure compound towards HepG2 and Chang liver cell lines**

MTT assay was used to assess the cytotoxicity of the isolated novel compound

from the diethyl ether extract of *T. chebula* fruit against HepG2 and Chang liver cells. The cell lines were initially obtained from the NCCS in Pune, India, and were kept in DMEM (Sigma Aldrich, USA) supplemented with L-glutamine, 10% fetal bovine serum (FBS), sodium bicarbonate, penicillin (100 U/mL), streptomycin (100  $\mu\text{g}/\text{mL}$ ), and amphotericin B (2.5  $\mu\text{g}/\text{mL}$ ). Cells were cultured in 25  $\text{cm}^2$  tissue culture flasks in a humidified 5%  $\text{CO}_2$  incubator (NBS Eppendorf, Germany) at 37 °C. Trypsinization was used to subculture the cells, and the cells were kept in Dulbecco's modified eagle medium (DMEM). The experiment was carried out three times in triplicate.

A 96-well plate was seeded with a total of  $2 \times 10^3$  cells. After a 24-h incubation period, the cells were treated with the compound at various concentrations (0.78-100  $\mu\text{g}/\text{mL}$ ). Negative control cells were untreated cells. The cells were treated and incubated for 24 h at 37 °C and 5%  $\text{CO}_2$ . After the chosen incubation time, 10  $\mu\text{L}$  MTT (5  $\text{mg}/\text{mL}$ ) was added to each well and the plates were incubated for 4 h. The formazan crystals were dissolved in 100  $\mu\text{L}$  of DMSO after the supernatants were removed. Using a microwell plate reader, the extent of MTT reduction was measured at 590 nm with a reference wavelength of 620 nm. Percentage cell viability was calculated by the following equation (13,14). All absorbance values have been adjusted against blank wells that only included growth media. The average absorbance of cells grown without the test compound was taken as 100% cell survival. Ascorbic acid was used as a positive control in this research.

$$\text{Cell viability (\%)} = \frac{\text{Absorbance of sample}}{\text{Absorbance of control}} \times 100$$

#### **Antigenotoxic effects of the isolated compound by Comet assay on HepG2 and Chang liver cells**

HepG2 and Chang liver cells were cultured at 37 °C in an atmosphere of 5%  $\text{CO}_2$ -95% air humidity. DMEM (Sigma Aldrich, USA) was used as the culture medium, which was supplemented with L-glutamine, 10% FBS, sodium bicarbonate, penicillin (100 U/mL), streptomycin (100  $\mu\text{g}/\text{mL}$ ), and amphotericin B (2.5  $\mu\text{g}/\text{mL}$ ). The cells were then seeded at a density of  $3 \times 10^4$  cells per well in a 6-well

plate for testing. The isolated compound was applied to the cells for 1 h at 37 °C. The compound concentration was chosen from a range of non-toxic concentrations determined by the MTT assay on both cell lines. DNA damage was induced for 15 min with 50 µM H<sub>2</sub>O<sub>2</sub> and then incubated for 24 h. The adherent cells were then trypsinized, centrifuged, and resuspended in ice-cold phosphate-buffered saline (PBS) before being thoroughly mixed with 50 µL of 0.5% low melting point agarose at pH 7.4 at 40 °C. Microscopic slides were cleared in flame after being rinsed with alcohol. The slides were frosted and then coated with 1% normal melting point agarose before being stored at 40 °C. A 1.6 mL sample was pipetted onto a frosted glass slide that had been pre-coated with a layer of 1% normal melting point agarose prepared in PBS and covered with a glass coverslip. The agarose was immediately chilled for 5 min to allow for complete agarose solidification. After removing the coverslip, the slides were immersed in a lysis solution (2.5 M NaCl, 100 mM Na<sub>2</sub>EDTA, 10 mM Tris, NaOH to pH 10, and 1% Triton X-100) at 4 °C for 1 h. DNA was allowed to unwind for 20 min in freshly prepared alkaline electrophoresis buffer (1 mM Na<sub>2</sub>EDTA, 0.3 N NaOH, pH 13). The slides were then placed in a horizontal electrophoresis tank and electrophoresis was performed at 12 V/cm for 20 min at a temperature of 40 °C. The slides were then washed three times with 1× Tris for 5 min with neutralizing buffer (0.4 M Tris-HCl buffer, pH 7.4) before staining with 20 µL ethidium bromide (20 µg/mL) (15,16).

### **Gene expression study**

#### *Culturing of cell lines*

Initially, the cell lines (HepG2 and Chang) procured from NCCS, Pune, India were maintained in DMEM (Sigma Aldrich, USA) supplemented with L-glutamine, 10% FBS, sodium bicarbonate, penicillin (100 U/mL), streptomycin (100 µg/mL), amphotericin B (2.5 µg/mL). The cells were continuously cultured in 25 cm<sup>2</sup> tissue culture flasks and kept at 37 °C in a humidified 5% CO<sub>2</sub> incubator (NBS Eppendorf, Germany).

### **RNA isolation**

After attaining 70% confluency, the cells ( $4 \times 10^5$  cells) were treated with the test compound for 1 h in a 6-well plate. Succeeding the incubation, all the samples were treated with H<sub>2</sub>O<sub>2</sub> for 15 min and the cells were subsequently incubated for 24 h. A set of untreated control cells was also kept synchronous with the treated cells. After the 24-h incubation, the media were removed aseptically and RNA was isolated. Total RNA was isolated using an RNA isolation kit according to the manufacturer's instructions (Invitrogen, USA; Product Code: 10296010). The disruption of cells and extraction of RNA were made with 200 µL of TRIzol solution followed by 200 µL of chloroform. The cells were vigorously shaken and incubated at room temperature for 3-5 min. After centrifugation at 14000 rpm for 15 min at 4 °C, 500 µL of 100% isopropanol was added and incubated for 10 min at room temperature. Thereon, the mixture was centrifuged again at 14000 rpm for 15 min at 4 °C. The supernatant was discarded, and the RNA was precipitated as a white pellet on the lower side of the tube. The resultant RNA pellet was washed with 200 µL of 70% ethanol (Merck, India) and centrifuged at 14000 rpm for 5 min at 4 °C. Ultimately, the pellets were dried and suspended in Tris-EDTA (TE) buffer. The purity and quantity of the total RNA were determined by RNA assay using Qubit version-3 (Thermo Scientific, USA).

### **cDNA synthesis and amplification**

The cDNA was synthesized using the Thermo Scientific Verso cDNA synthesis kit (Product Code: AB-1453/A). To an RNase-free tube, add about 4 µL of 5× cDNA synthesis buffer, 2 µL of deoxynucleotide triphosphate (dNTP) mix, 1 µL of anchored oligo dT, 1 µL of RT enhancer, 1 µL of verso enzyme mix, and 5 µL of RNA template (1 ng of total RNA), then the total reaction volume was made up to 20 µL with the addition of sterile distilled water and mixed gently. The cDNA synthesis was executed in the thermal cycler (Eppendorf master cycler). The following cycling conditions were employed for 30 min at 42 °C and 2 min at 95 °C. Temperature conditions of cDNA synthesis are given in Table 1.

**Table 1.** Temperature conditions of cDNA synthesis.

Steps	Temperature (°C)	Time (min)	Number of cycles
cDNA synthesis	42	30	1
Inactivation	95	2	1

**Table 2.** Primers and their annealing temperatures.

Gene	Forward		Reverse	
	Sequence (5' > 3')	T <sub>m</sub> (°C)	Sequence (5' > 3')	T <sub>m</sub> (°C)
NEIL1	GCAGAATAACTGTGTGCCGCT	59.82	ACCCTGCTAGATGTCCAAGTATT	61.01
OGG1	GTGCCCGTTACGTGAGTGTGCCAGTGC	69.54	AGAGAAGTGGGAATGGAGGGGAAGGTG	69.51
B-Actin	TCACCCACACTGTGCCCATCTACGA(25)	66.3	CAGCGGAACCGCTCATTGCCAATGG(25)	67.9

NEIL1, Endonuclease VIII-like 1; OGG1, 8-oxoguanine DNA glycosylase; T<sub>m</sub>, melting temperature.

**Table 3.** Steps of polymerase chain reaction amplification.

Step	Temperature (°C)	Time	Number of cycles
Initial denaturation	95	3 s	1
Denaturation	95	30 s	
Annealing	50-65	30 s	25-40
Extension	72	1 min/kb	
Final extension	72	15 min	1

The amplification was performed by utilizing a Thermo Scientific amplification kit. The components from the kit were added to each PCR vial. The 50  $\mu$ L reaction mixture consisted of 25  $\mu$ L of PCR master mix, 2  $\mu$ L of forward and reverse primers and 5  $\mu$ L of template DNA. The components were made up to 50  $\mu$ L with nuclease-free sterile distilled water. The PCR was programmed after standardization, and after amplification, the PCR products were segregated using agarose gel electrophoresis. Table 2 outlines the details of primers and their annealing temperatures. However, Table 3 shows the steps of PCR amplification.

A gel was prepared using 1.5% agarose in 1 $\times$  TE buffer by adding 6  $\mu$ L of 10 mg/mL ethidium bromide. Then, the gel was loaded with samples and accomplished the electrophoresis procedure at 50V for 30 min. The stained gel was then viewed under the gel documentation system (E gel imager, Invitrogen, USA), and the intensity of the band and the level of expression were calculated using the software Image J.

### Statistical analyses

Statistical analysis of the data was performed by SPSS version 20.0 (SPSS Inc,

Chicago, IL, USA). The outcome of the investigations is expressed as the mean  $\pm$  SD of three independent experimentations. The student t-test and one-way ANOVA test followed by Tukey test were used to find out the statistical significance. Differences were considered statistically significant at  $P < 0.05$ .

## RESULTS

### Structural elucidation of the novel isolated compound

Various fractions collected from the column chromatography were pooled based on the TLC profile. All pooled fractions were tested for the occurrence of flavonoids. Afterward, the fractions were subjected to *in vitro* antioxidant studies (data not shown). Fraction 5, which yielded a pure compound and recorded significant antioxidant activity, was subjected to detailed structural elucidation. The pure compound yielded in fraction 5 appeared as a yellow solid, and its melting point was observed at 235 °C. The UV-visible spectrum of the compound with  $\lambda_{\max}$  at 254 and 365 is shown in Fig. 1. Absorption bands at 254 and 365 nm indicated the presence of an aromatic ring and carbonyl group, respectively. The higher value of the carbonyl group may be due to the



interaction of lone pairs of oxygen in the carbonyl and ester groups.

The FT-IR spectrum of the compound is depicted in Fig. 2A. The details of IR bands observed in the spectrum along with the structural details are given in Table 4.

$^1\text{H}$  NMR spectra of the isolated compound are depicted in Fig. 2B. Phenolic O-H appeared at 9.3 ppm estimating the presence of two phenolic groups in the compound. The peaks detected between 7.0 and 7.4 ppm have marked the presence of five aromatic hydrogen atoms present in two rings. Peaks at 6.8-6.9 ppm indicated the presence of unsaturated moieties in aliphatic chains connected to the core structure. NMR peaks from 0.84-2.1 ppm pointed out the presence of aliphatic saturated hydrogens in the chain.

Based on UV-Vis, FT-IR, and NMR spectra, the following information was derived:

The core structure contained polyaromatic rings; the aromatic rings were substituted with the functional groups at various positions; at least, two phenolic hydrogens were present in the core; the presence of a C=O group was confirmed; unsaturation of the alkyl chain was also observed; and the presence of ether linkage connected between aliphatic and aromatic moieties was confirmed.

Given the obtained data, the mass spectra (as shown in Fig. 2C) have been interpreted as a confirmatory analysis for the elucidation of the compound. The structural elucidation was supported by the data for this family, available in the literature (17).

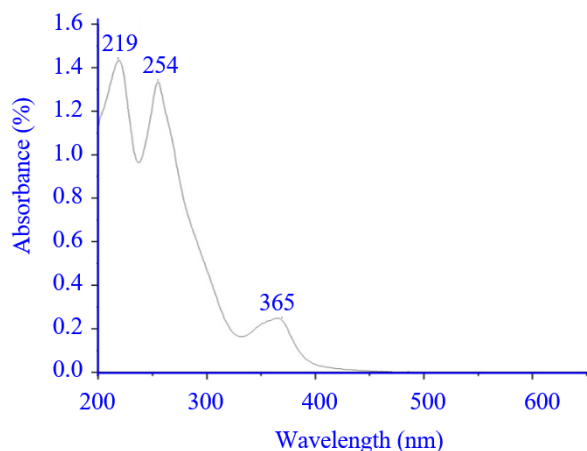
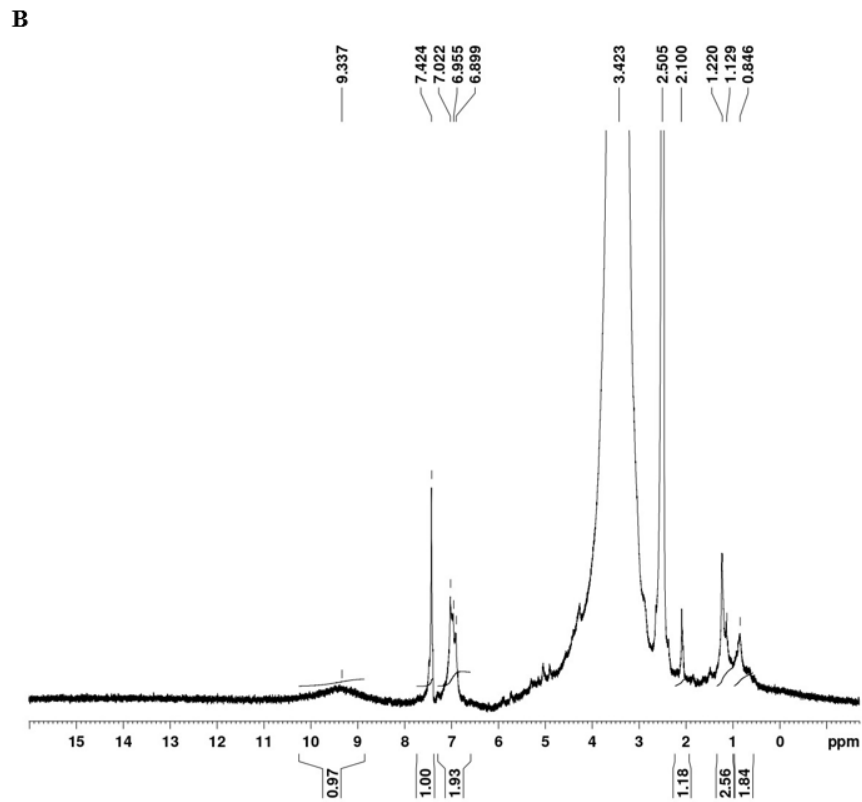
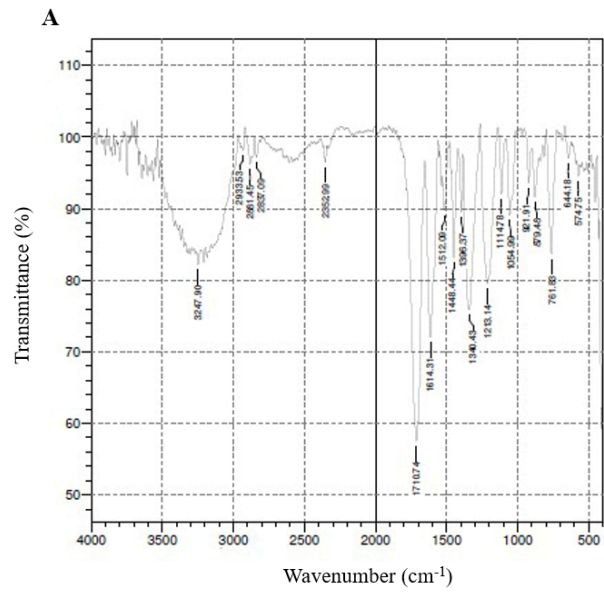


**Fig. 1.** UV-visible spectrum of the pure compound isolated from *Terminalia chebula* fruit.

**Table 4.** Description of the spectrum of compound isolated from *Terminalia chebula* fruit obtained by Fourier transform infrared spectroscopy.

No	Band frequency (cm <sup>-1</sup> )	Description
1	3247	C-H stretching vibrations of alkene
2	2933	C-H stretching vibrations of CH <sub>3</sub>
3	2881	C-H stretching vibrations of CH <sub>2</sub>
4	2837	C-H stretching vibrations of CH
5	1712	C=O stretching
6	1614	C=C stretching
7	1512-1448	C-C stretching of the aromatic ring
8	1340	C-O-C stretching band
9	1213	Aromatic C-O of the phenyl group
10	1114	Aliphatic C-O of the phenyl group
11	761	Poly substitution on aromatic rings



C

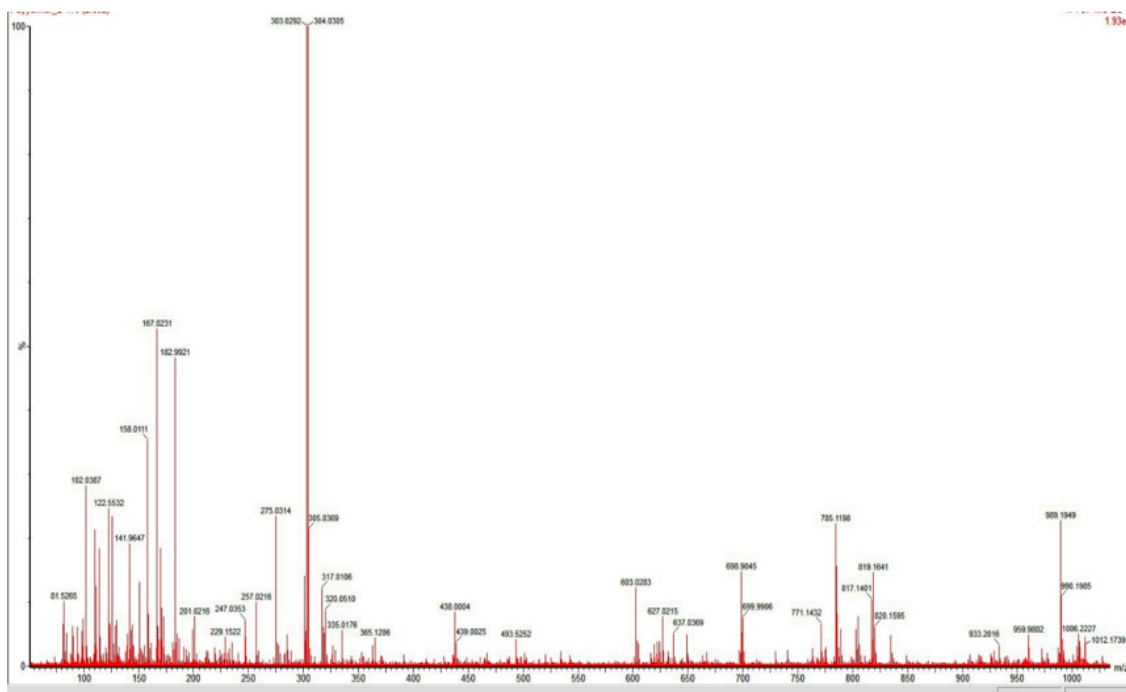


**Fig. 2.** (A) Fourier transform infrared spectroscopy, (B) proton nuclear magnetic resonance spectroscopy, and (C) mass spectra of the compound isolated from *Terminalia chebula* fruit.

The base peak at 303 shows the core structure of the compound, which consists of quercetin. The mass spectra were explained on this basis and elucidated for other substitutions of quercetin. This was confirmed by the fractions of 229 (fragmentation of the second benzene ring (B) from the parent compound) and 73 for the fragmented part. From the mass spectra values, it was observed that the compound existed sometimes as a dimer. The fragmentation pattern is shown in Table 5.

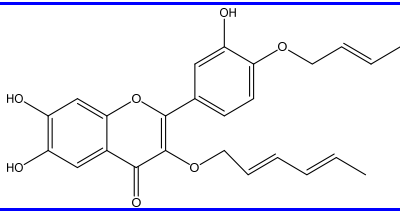
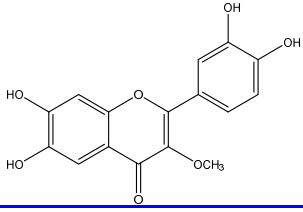
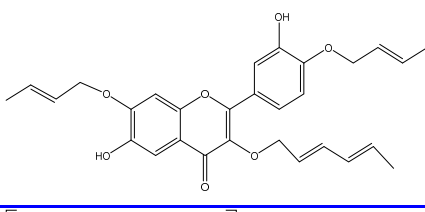
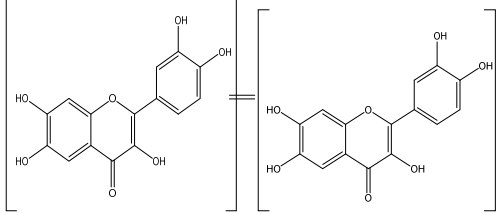
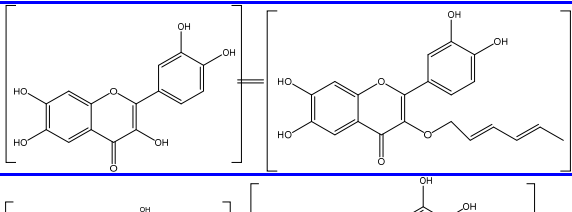
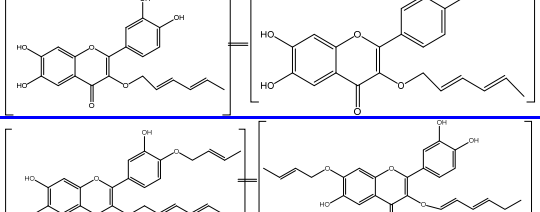
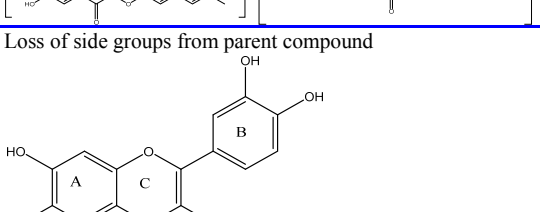
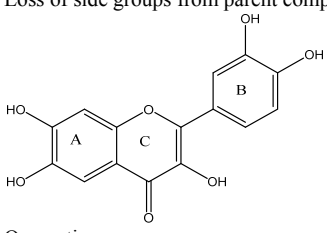
The substituents were placed preferably at positions 7, and 4' having the shortest substituent, and 3' having the longest substituent. This might be due to avoiding the steric hindrance. Figure 3 depicts the chemical structure of the isolated compound, a novel quercetin derivative known as 7-(hydroxyl alkyl substituted)-2-(4(hydroxyl alkyl substituted)-3-hydroxyphenyl)-3-(hydroxyl alkyl substituted)-6-hydroxy-4H-chromen-4-one.

### ***Cytotoxic effects of novel quercetin derivative on HepG2 and Chang liver cells***

The cytotoxic activity of isolated flavonoid on HepG2 cells after 24-h incubation was evaluated by MTT assay. The cell viability (%) was calculated in each concentration and the outcomes are depicted in Table 6. The cytotoxicity study aimed to determine the concentration that could elicit minimum cytotoxicity towards the cell line to be further used for antigenotoxic and expression studies. However, there was no cytotoxicity observed for the compound at their lower concentrations. The compound showed a moderate cytotoxic effect even at the high concentration (100  $\mu\text{g/mL}$ ). The compound showed a cell viability of 90% at the concentration of 1.56  $\mu\text{g/mL}$  for HepG2 and 3.12  $\mu\text{g/mL}$  for Chang liver cells, and this concentration was selected for the compound for antigenotoxic and expression studies.



**Table 5.** Description of mass spectra of pure compound isolated from *Terminalia chebula* fruit.

Sl. No.	Peak value	Structure	Existing peaks
1.	438		(303 + 95 - 15 + 55)
2.	317		(303 + 15)
3.	493		(303 + 95 - 15 + 55 + 55)
4.	603		(303 × 2 = 606)
5.	698		(606 + 95)
6.	785		(606 + 95 + 95)
7.	933		(438 + 438 + 55)
Loss of side groups from parent compound			
8.	303		303
9.	285	Loss of OH from quercetin	303 - 17

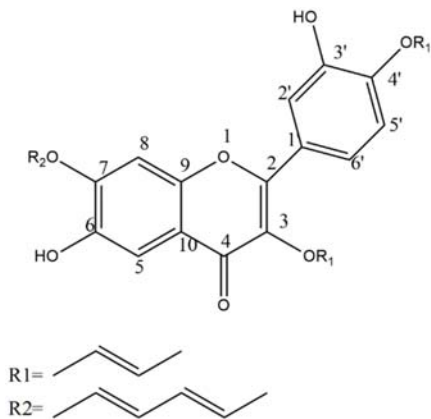


**Fig. 3.** Chemical structure of novel quercetin derivative isolated from *Terminalia chebula* fruit.

**Table 6.** The effect of flavonoid compound isolated from the fruit of *Terminalia chebula* on the viability of HepG2 and Chang liver cell by MTT assay. Results are expressed as mean  $\pm$  SEM of six experiments. \* $P < 0.05$  Indicates statistically significant differences between two cell lines in each concentration.

Concentration ( $\mu\text{g/mL}$ )	Cell viability (%)	
	HepG2 cells	Chang liver
100	64.71 $\pm$ 0.38	45.32 $\pm$ 0.07
50	65.70 $\pm$ 0.87	57.00 $\pm$ 0.07
25	70.96 $\pm$ 0.33	60.12 $\pm$ 0.14
12.5	75.96 $\pm$ 0.86	73.00 $\pm$ 0.07
6.25	85.74 $\pm$ 0.86	81.79 $\pm$ 0.12
3.12	89.91 $\pm$ 0.99	92.48 $\pm$ 0.11*
1.56	92.35 $\pm$ 1.27*	95.44 $\pm$ 0.16*
0.78	94.37 $\pm$ 1.47*	97.68 $\pm$ 0.87*

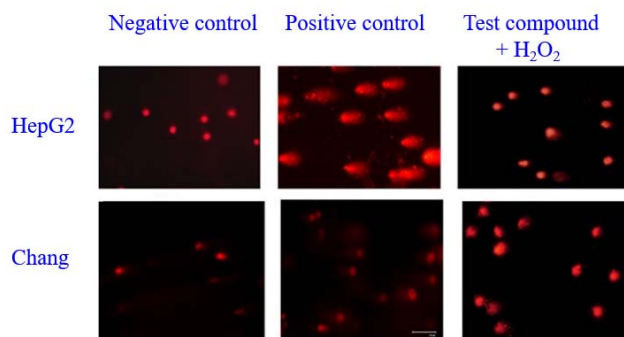


**Fig. 4.** The extent of DNA damage in HepG2 and Chang liver cells treated with the novel quercetin derivative isolated from *Terminalia chebula*. The untreated cells were designated as the negative control group while those treated with  $\text{H}_2\text{O}_2$  were considered the positive control group.

#### Antigenotoxic effects of novel quercetin derivative on HepG2 and Chang liver cells

The antigenotoxic effect of the isolated compound on HepG2 and Chang liver cells was evaluated using an alkaline Comet assay (Fig. 4). The level of DNA damage was measured by comet length, tail length, and tail DNA percentage. The isolated quercetin compound recorded significant DNA damage in HepG2 and Chang liver cells. Table 7 shows the data for the antigenotoxicity calculation. Just before being exposed to  $\text{H}_2\text{O}_2$ , the cells were incubated for 1 h with a non-toxic concentration of the isolated compound. The cells were subsequently subjected to various concentrations of  $\text{H}_2\text{O}_2$  and incubated for

varying lengths of time. Because  $\text{H}_2\text{O}_2$  at 50  $\mu\text{M}$  for 15 min was found to be an adequate amount to induce a high level of DNA impairment, it was chosen for further research. Comet length, tail length, and tail DNA percentage were all measured in 100 cells per sample.

When the cells were exposed to  $\text{H}_2\text{O}_2$ , the comet length, tail length, and tail DNA percentage increased in comparison with the untreated cells. When the cells were pre-treated with the isolated compound, these parameters were found to decrease. Overall, the compound demonstrated significant protection against  $\text{H}_2\text{O}_2$ -induced DNA damage in both cells at the non-toxic concentration tested.

**Table 7.** Level of DNA damage in normal, control, and the isolated phenolic compound on HepG2 and Chang liver cells. Results are expressed as mean  $\pm$  SEM, n = 6. \* $P$  < 0.05 Indicates significant differences compared to untreated cells as negative control.

Cell lines	Group	Comet length	Tail length	Tail DNA (%)
HepG2	Negative control	24.83 $\pm$ 5.8	1.66 $\pm$ 0.05	1.23 $\pm$ 0.03
	Positive control (H <sub>2</sub> O <sub>2</sub> )	94 $\pm$ 1.8*	27 $\pm$ 2.2*	20.6 $\pm$ 3.1*
	Test compound+ H <sub>2</sub> O <sub>2</sub>	70.86 $\pm$ 4.6*	4.66 $\pm$ 0.2*	4.4 $\pm$ 0.8*
Chang liver	Normal	23.12 $\pm$ 4.2	1.21 $\pm$ 0.0	1.5 $\pm$ 0.02
	H <sub>2</sub> O <sub>2</sub>	92.45 $\pm$ 3.5*	28.86 $\pm$ 2.1*	27.34 $\pm$ 2.3*
	Compound	56.97 $\pm$ 4.1*	4.2 $\pm$ 0.2*	4.2 $\pm$ 0.08*

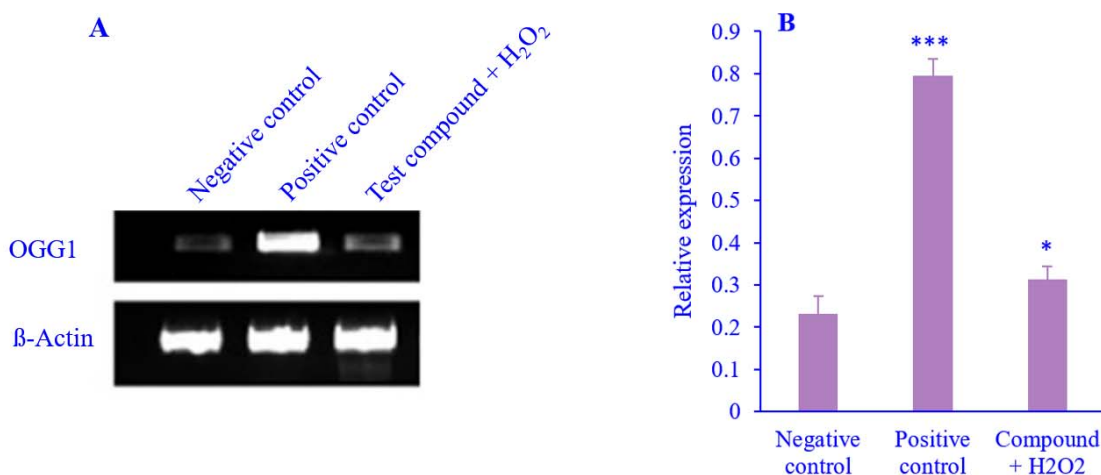


**Fig. 5.** The effect of H<sub>2</sub>O<sub>2</sub> and test compound (novel quercetin derivative) isolated from *Terminalia chebula* on the relative expression of OGG1 in HepG2 cells. (A) Gel electrophoresis image OGG1 and  $\beta$  actin mRNA expression and (B) graphical representation of the relative expression of OGG1. The untreated cells were designated as the negative control group while those treated with H<sub>2</sub>O<sub>2</sub> were considered the positive control group. Results are expressed as mean  $\pm$  SEM; n = 6. \* $P$  < 0.05 and \*\*\* $P$  < 0.001 indicate significant differences relative to negative control.

#### Effect of novel quercetin derivative on gene expression level in HepG2 and Chang liver cells

A gene expression study of an isolated phenolic compound in HepG2 and in Chang liver cells was performed by RT-PCR. The expression levels of OGG1 and NEIL1 in HepG2 cells (Figs. 5 and 6) were observed to be the highest under the H<sub>2</sub>O<sub>2</sub> stress condition (0.796 and 1.002, respectively), indicating that these genes have an activating effect under these conditions. As shown in the figures, after treatment with the isolated compound, the expression level of OGG1 and NEIL1 was found to significantly decrease when compared to the H<sub>2</sub>O<sub>2</sub>-treated group. The isolated compound reduced OGG1 and NEIL1 levels in

the HepG2 cell by 60.5% and 70.25% of those of the positive control groups, respectively.

In the case of untreated Chang liver cells, the expression levels of OGG1 and NEIL1 were found to be 0.994 and 0.323, respectively. Treating the cells with H<sub>2</sub>O<sub>2</sub> at 50 M for 15 min resulted in high levels of OGG1 and NEIL1 expression. The pre-treatment with the isolated compound reduced the OGG1 and NEIL1 gene expression levels to 44.5% and 69.7% of that of the positive control groups, respectively (Figs. 7 and 8).

Overall results of the expression studies demonstrated that the isolated flavonoid compound can normalize the expression level of OGG1 and NEIL1.

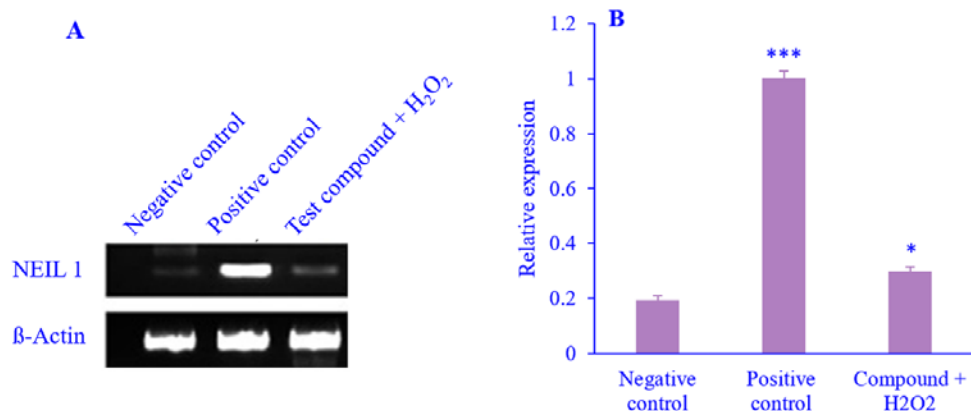


**Fig. 6.** The effect of H<sub>2</sub>O<sub>2</sub> and test compound (novel quercetin derivative) isolated from *Terminalia chebula* on the relative expression of NEIL1 in HepG2 cells. (A) Gel electrophoresis image for NEIL1 and β actin mRNA expression levels and (B) graphical representation of the relative expression of NEIL1. The untreated cells were designated as the negative control group while those treated with H<sub>2</sub>O<sub>2</sub> were considered the positive control group. Results are expressed as mean ± SEM; n = 6. \**P* < 0.05 and \*\*\**P* < 0.001 indicate significant differences relative to the negative control.

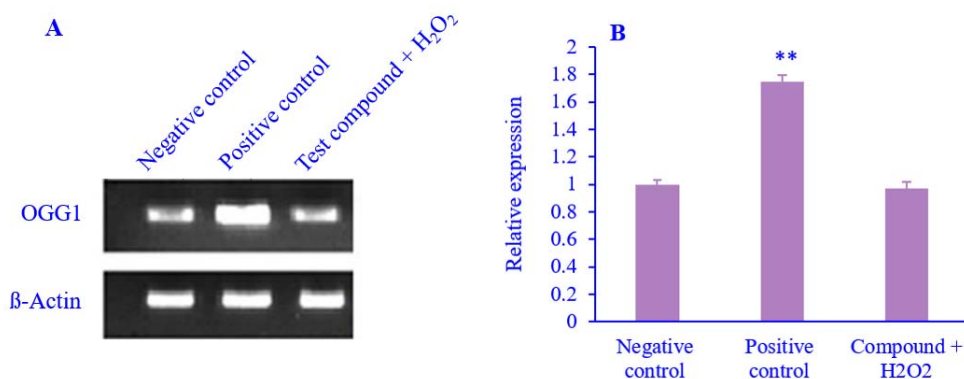


**Fig. 7.** The effect of H<sub>2</sub>O<sub>2</sub> and test compound (novel quercetin derivative) isolated from *Terminalia chebula* on the relative expression of OGG1 in Chang liver cells. (A) Gel electrophoresis image for OGG1 and β actin mRNA expression levels and (B) graphical representation of the relative expression of OGG1. The untreated cells were designated as the negative control group while those treated with H<sub>2</sub>O<sub>2</sub> were considered the positive control group. Results are expressed as mean ± SEM; n = 6. \*\**P* < 0.01 indicates significant differences relative to negative control.

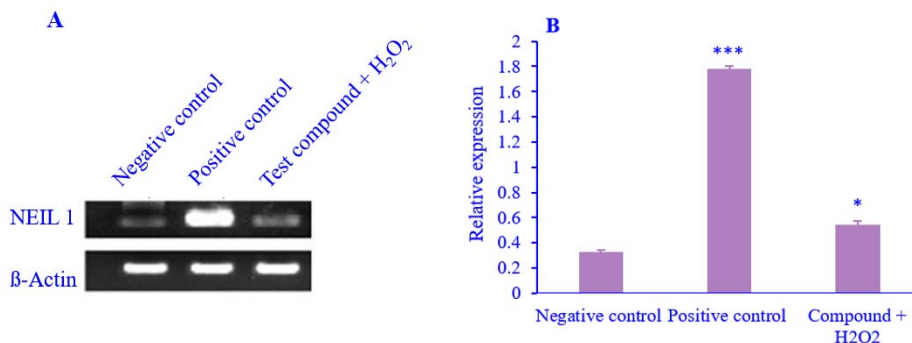


**Fig. 8.** The effect of H<sub>2</sub>O<sub>2</sub> and test compound (novel quercetin derivative) isolated from *Terminalia chebula* on the relative expression of NEIL1 in Chang liver cells. (A) Gel electrophoresis image for NEIL1 and β actin mRNA expression levels and (B) graphical representation of the relative expression of NEIL1. The untreated cells were designated as the negative control group while those treated with H<sub>2</sub>O<sub>2</sub> were considered the positive control group. Results are expressed as mean ± SEM; n = 6. \**P* < 0.05 and \*\*\**P* < 0.001 indicate significant differences relative to negative control.

## DISCUSSION

Oxidative damage to DNA due to ROS/reactive nitrogen species has been described to have a deleterious effect on the human body. A remarkable level of DNA damage has been widely accepted as the major cause of many maladies like cancer, neurodegenerative diseases, diabetes, and premature aging. Hence, the protection of DNA from the harmful effect of ROS has significant implications for the prevention of the above-mentioned diseases (18). An efficient antioxidative system can scavenge or detoxify the excess ROS; they comprise enzymatic (superoxide dismutase, catalase) and non-enzymatic components (glutathione) (19). Additionally, the cells have a network of DNA repair pathways to recognize and repair different types of lesions, and in this way, the equilibrium between DNA damage and repair is attained. However, erratically, the equilibrium can be disrupted; those systems would not be enough to counteract ROS action (20).

The liver is the chief organ attacked by ROS (21,22). The liver functions as one of the most indispensable organs in the body, playing a fundamental role in the regulation of diverse processes such as metabolism, secretion, storage, and detoxification of endogenous and exogenous substances (23,24). Considering these major functions, liver diseases account for a principal threat to public health. Moreover, it has been reported that the currently available synthetic drugs for hepatic diseases also cause supplementary damage to DNA (25,26). The present study delved into the promising DNA protective activity of a novel flavonoid isolated from *T. chebula* fruit on hepatic cells.

In this work, a novel flavonoid, (quercetin derivative) 7-(but-2-en-1-yloxy)-2-(4(but-2-en-1-yloxy)-3-hydroxyphenyl)-3-(hexa-2,4-dien-1-yloxy)-6-hydroxy-4H-chromen-4-one, isolated from *T. chebula* fruit was probed for the cytotoxic and protective effects on oxidative DNA damage in two cell lines, HepG2 and Chang liver cell. The results of the MTT assay confirmed that the isolated compound was relatively non-toxic at medium and lower concentrations to the cell lines. In the

antigenotoxic activity study, we discovered that the isolated flavonoid had antigenotoxic properties against H<sub>2</sub>O<sub>2</sub>-induced damage in hepatic cells when administered prior to the genotoxic agents. Ascorbic acid was used as a positive control in this research. The data compiled from this study using comet analysis showed that in the presence of flavonoids, the number of comet-bearing cells was markedly reduced in each cell. At this time, we do not know the precise mechanism(s) underlying the antigenotoxic activity. However, the detected antigenotoxic properties of isolated phenolic molecules may be related to the synergistic action of mechanisms such as restriction of toxin penetration into cells, direct deactivation of toxins by scavenging, stimulation of detoxification, increase or decrease in cytotoxicity, activation of DNA repair enzymes, and structure-activity interaction (27-29). The detected protective effect of the molecule on the cell lines HepG2 and Chang liver may correspond to synergistic participation of the above-mentioned mechanism(s).

Gene expression analysis was carried out on the isolated compound in order to divulge whether this compound exerts DNA protection against oxidative damage either by enhancing DNA repair activity or simply by preventing oxidative damage due to its antioxidant activity. We have selected the best concentration for the isolated compound, which did not induce any toxicity to the cells, and the suitable condition (50 µM for 15 min) for hydrogen peroxide that would induce a significant amount of DNA damage without affecting the viability of the cell. Recognizing the facts mentioned above, we have proceeded to investigate the protective action of an isolated flavonoid compound against H<sub>2</sub>O<sub>2</sub>-induced oxidative DNA damage. Similar concentrations of H<sub>2</sub>O<sub>2</sub> have been used in other studies with HepG2 cells (30).

H<sub>2</sub>O<sub>2</sub> predominantly induces single-strand breaks in DNA, which could be repaired by the BER pathway (31). OGG1 and NEIL1 are the two major DNA glycosylases involved in the BER pathway. The potential of the isolated compound to protect DNA from strand breaks was investigated by the RT-PCR method. We

have detected an increase in the mRNA levels of OGG1 and NEIL1 in two cell lines after H<sub>2</sub>O<sub>2</sub> treatment. The isolated compound decreased the level of OGG1 and NEIL1. On DNA protection, after a short period of treatment (1 h) with isolated flavonoids, it has exhibited a maximum protective effect against H<sub>2</sub>O<sub>2</sub>-induced DNA damage in HepG2 and Chang liver cells. Earlier, Kim *et al.* reported that 7,8-dihydroxyflavone induces OGG1 expression via the PI3K-Akt pathway and protects cells against oxidative DNA base damage by activating DNA repair systems (31). Kang *et al.* also demonstrated that 7,8-dihydroxyflavone augments the cellular antioxidant defense capacity through activation of the Nrf2/H-1 pathway, which also involves the activation of the PI3K/Akt and ERK pathways, thereby protecting C2C12 myoblasts from H<sub>2</sub>O<sub>2</sub>-induced oxidative cytotoxicity (32).

The outcome of an isolated compound on recovery from DNA oxidative damage can be explained by two mechanisms, either the capability to enhance the activity of repair enzymes or (ii) absolute and direct protection against oxidation (33). The strong protective effect against oxidative damage for the pre-treated sample suggested that the isolated compound acted through a second mechanism. Protection of DNA from strand breakage together with the increased antioxidant activity exerted by this compound can account for the significant reduction of endogenous oxidative damage.

## CONCLUSIONS

Contemplating the empirical evidence, we can culminate that the isolated compound, 7-(but-2-en-1-yloxy)-2-(4(but-2-en-1-yloxy)-3-hydroxyphenyl)-3-(hexa-2,4-dien-1-yloxy)-6-hydroxy-4H-chromen-4-one, has effectively normalized the expression levels of OGG1 and NEIL1 when compared to the untreated cells. The action of the isolated compound seems to be associated with its efficacy on ROS scavenging property, which has major implications for the prevention of H<sub>2</sub>O<sub>2</sub>-induced strand breakages. This study corroborated the strong hepatoprotective action of a novel flavonoid isolated from *T. chebula*.

The active ingredients that trigger these antioxidative activities, however, are currently unknown. Further pharmacological studies must be supplemented by *in vivo* studies to gain a better understanding of the novel compound's mechanism of action, which may pave the way for the invention of an entirely novel therapeutic natural drug.

## Acknowledgments

This study was supported by the Council of Scientific and Industrial Research (Sr. No. 1061210077), India. We are also thankful to Mrs. Vidya, Calicut University, Kerala, India for the service provided for cell line studies.

## Conflict of interest statement

The authors declared no conflict of interest in this study.

## Authors' contributions

K. Soumya performed all the experiments; K.R. Haridas performed structural characterization of the compound; J. James supported conducting experimental parts; S. Sudheesh conceived the original idea, supervised, and funded the project. The final version of the article was read and approved by all authors.

## REFERENCES

1. Maynard S, Schurman SH, Harboe C, de Souza-Pinto NC, Bohr M VA. Base excision repair of oxidative DNA damage and association with cancer and aging. *Carcinogenesis*. 2009;30(1):2-10. DOI: 10.1093/carcin/bgn250.
2. Poetsch AR, Boulton SJ, Luscombe NM. Genomic landscape of oxidative DNA damage and repair reveals regioselective protection from mutagenesis. *Genome Biol*. 2018;19(1):215,1-23. DOI: 0.1186/s13059-018-1582-2.
3. Lee MR, Kim SH, Cho HJ, Lee KY, Moon AR, Jeong HG, *et al.* Transcription factors NF-YA regulate the induction of human OGG1 following DNA-alkylating agent methylmethane sulfonate (MMS) treatment. *J Biol Chem*. 2004;279(11):9857-9866. DOI: 10.1074/jbc.M311132200.
4. Whitaker AM, Schaich MA, Smith MR, Flynn TS, Freudenthal BD. Base excision repair of oxidative DNA damage: from mechanism to disease. *Front Biosci*. 2017;22(9):1493-1522. DOI: 10.2741/4555.
5. Aguiar PHN, Furtado C, Repolês BM, Ribeiro GA, Mendes IC, Peloso EF, *et al.* Oxidative stress and



- DNA lesions: the role of 8-oxoguanine lesions in *Trypanosoma cruzi* cell viability. PLoS Negl Trop Dis. 2013;7(6):e2279,1-13.  
DOI: 10.1371/journal.pntd.0002279.
6. Hu J, de Souza-Pinto NC, Haraguchi K, Hogue BA, Jaruga P, Greenberg MM, et al. Repair of formamidopyrimidines in DNA involves different glycosylases: role of the OGG1, NTH1, and NEIL1 enzymes. J Biol Chem. 2005;280(49):40544-40551.  
DOI: 10.1074/jbc.M508772200.
  7. Saleem A, Husheem M, Härkönen P, Pihlaja K. Inhibition of cancer cell growth by crude extract and the phenolics of *Terminalia chebula* retz. fruit. J Ethnopharmacol. 2002;81(3):327-336.  
DOI: 10.1016/S0378-8741(02)00099-5.
  8. Soumya K, Haridas KR, James J, Kumar VBS, Edatt L, Sudheesh S. Study of *in vitro* antioxidant and DNA damage protection activity of a novel luteolin derivative isolated from *Terminalia chebula*. J Taibah Univ Sci. 2019;13:755-763.  
DOI: 10.1080/16583655.2019.1630892.
  9. Soumya K, Jesna J, Sudheesh S. Screening study of three medicinal plants for their antioxidant and cytotoxic activity. Int J Pharm Sci Res. 2018;9(9):3781-3787.  
DOI: 10.13040/IJPSR.0975-8232.9(9).3781-87.
  10. Malekzadeh F, Ehsanifar H, Shahamat M, Levin M, Colwell RR. Antibacterial activity of black myrobalan (*Terminalia chebula* Retz) against helicobacter pylori. Int J Antimicrob Agents. 2001;18(1):85-88.  
DOI: 10.1016/S0924-8579(01)00352-1.
  11. Dutta BK, Rahman I, Das TK. Antifungal activity of Indian plant extracts. Mycoses. 1998;41(11-12):535-536.  
DOI: 10.1111/j.1439-0507.1998.tb00718x.
  12. Shabrina R, Elya B, Noviani A. Antioxidant activities of fractions from ethyl acetate extracts of *Garcinia fruticosa* lauterb leaves. Int J Appl Pharm. 2018;10(1):44-50.  
DOI: 10.22159/ijap.2018.v10s1.10.
  13. Swamy SM, Tan BK. Cytotoxic and immunopotentiating effects of ethanolic extract of *Nigella sativa* L. seeds. J Ethnopharmacol. 2000;70(1):1-7.  
DOI: 10.1016/S0378-8741(98)00241-4.
  14. Auddy B, Ferreira M, Blasina F, Lafon L, Arredondo F, Dajas F, et al. Screening of antioxidant activity of three indian medicinal plants, traditionally used for the management of neurodegenerative diseases. J Ethnopharmacol. 2003;84(2-3):131-138.  
DOI: 10.1016/S0378-8741(02)00322-7.
  15. Kang C, Lee H, Yoo YS, Hah DY, Kim CH, Kim E, et al. Evaluation of oxidative DNA damage using an alkaline single cell gel electrophoresis (SCGE) comet assay, and the protective effects of N-acetylcysteine amide on zearalenone-induced cytotoxicity in chang liver cells. Toxicol Res. 2013;29(1):43-52.  
DOI: 10.5487/TR.2013.29.1.043.
  16. Leandro LF, Munari CC, Sato VLFL, Alves JM, de Oliveira PF, Mastrocola DFP, et al. Assessment of the genotoxicity and antigenotoxicity of (+)-usnic acid in V79 cells and Swiss mice by the micronucleus and comet assays. Mutat Res. 2013;753(2):101-106.  
DOI: 10.1016/j.mrgentox.2013.03.006.
  17. Lei YX, Lu Q, Shao C, He CC, Lei ZN, Lian YY. Expression profiles of DNA repair-related genes in rat target organs under subchronic cadmium exposure. Genet. Mol. Res. 2015;14(1):515-524.  
DOI: 10.4238/2015.January.26.5.
  18. Pilařová V, Kuda L, Vlčková HK, Nováková L, Gupta S, Kulkarni M, et al. Carbon dioxide expanded liquid: an effective solvent for the extraction of quercetin from South African medicinal plants. Plant Methods. 2022;18(1):87,1-13.  
DOI: 10.1186/s13007-022-00919-6.
  19. Silva JP, Gomes AC, Proença F, Coutinho OP. Novel nitrogen compounds enhance protection and repair of oxidative DNA damage in a neuronal cell model: comparison with quercetin. Chem Biol Interact. 2009;181(3):328-337.  
DOI: 10.1016/j.cbi.2009.07.024.
  20. Ramos AA, Azqueta A, Pereira-Wilson C, Collins AR. Polyphenolic compounds from salvia species protect cellular DNA from oxidation and stimulate DNA repair in cultured human cells. J Agric Food Chem. 2010;58(12):7465-7471. DOI: 10.1021/jf100082p.
  21. García-Rodríguez A, Gosálvez J, Agarwal A, Roy R, Johnston S. DNA damage and repair in human reproductive cells. Int J Mol Sci. 2019;20(1):31,1-22.  
DOI: 10.3390/ijms20010031.
  22. Li S, Tan HY, Wang N, Zhang ZJ, Lao L, Wong CW, et al. The role of oxidative stress and antioxidants in liver diseases. Int J Mol Sci. 2015;16(11):26087-26124.  
DOI: 10.3390/ijms161125942.
  23. Madrigal-Santillán E, Madrigal-Bujaidar E, Álvarez-González I, Sumaya-Martinez MT, Gutiérrez-Salinas J, Bautisa M, et al. Review of natural products with hepatoprotective effects. World J Gastroenterol. 2014;20(40):14787-14804.  
DOI: 10.3748/wjg.v20.i40.14787.
  24. Srivastava R, Srivastava P. Hepatotoxicity and the role of some herbal hepatoprotective plants in present scenario. Global J Dig Dis. 2018;3:1-4.  
DOI: 10.4172/2472-1891.100034.
  25. Linares V, Alonso V, Albina ML, Bellés M, Sirvent JJ, Domingo JL, et al. Lipid peroxidation and antioxidant status in kidney and liver of rats treated with sulfasalazine. J Toxicol. 2009;256(3):152-156.  
DOI: 10.1016/j.tox.2008.11.010.
  26. Kilani-Jaziri S, Bhourri W, Skandrani I, Limem I, Chekir-Ghedira L, Ghedira K. Phytochemical, antimicrobial, antioxidant and antigenotoxic potentials of *Cyperus rotundus* extracts. S. Afr. J. Bot. 2011;77(3):767-776.  
DOI: 10.1016/j.sajb.2011.03.015.
  27. Prajitha V, Thoppi J.E. Genotoxic and antigenotoxic potential of the aqueous leaf extracts of *Amaranthus spinosus* Linn. using *Allium cepa* assay. S Afr J Bot. 2016;102:18-25.  
DOI: 10.1016/j.sajb.2015.06.018.

28. Prieto AM, dos Santos AG, Oliveira APS, Cavalheiro AJ, Silva DHS, Bolzani VS, *et al.* Assessment of the chemopreventive effect of casearin B, a clerodane diterpene extracted from *Casearia sylvestris* (Salicaceae). *Food Chem Toxicol.* 2013;53:153-159. DOI: 10.1016/j.fct.2012.11.029.
29. Benhusein GM, Mutch E, Aburawi S, Williams FM. Genotoxic effect induced by hydrogen peroxide in human hepatoma cells using comet assay. *Libyan J Med.* 2010;5:1-6. DOI: 10.3402/ljm.v5i0.4637.
30. Ismail IH, Nyström S, Nygren J, Hammarsten O. Activation of ataxia telangiectasia mutated by DNA strand break-inducing agents correlates closely with the number of DNA double strand breaks. *J Biol Chem.* 2005;280(6):4649-4655. DOI: 10.1074/jbc.M411588200.
31. Kim KC, Lee IK, Kang KA, Cha JW, Cho SJ, Na SY, *et al.* 7,8-Dihydroxyflavone suppresses oxidative stress-induced base modification in DNA via induction of the repair enzyme 8-oxoguanine DNA glycosylase-1. *Biomed Res Int.* 2013;2013:863720,1-10. DOI: 10.1155/2013/863720.
32. Kang JS, Choi IW, Han MH, Kim GY, Hong SH, Park C, *et al.* The cytoprotective effects of 7,8-dihydroxyflavone against oxidative stress are mediated by the upregulation of Nrf2-dependent HO-1 expression through the activation of the PI3K/Akt and ERK pathways in C2C12 myoblasts. *Int J Mol Med.* 2015;36(2): 501-510. DOI: 10.3892/ijmm.2015.2256.
33. Silva JP, Gomes AC, Coutinho OP. Oxidative DNA damage protection and repair by polyphenolic compounds in PC12 cells. *Eur J Pharmacol.* 2008;601(1-3):50-60. DOI: 10.1016/j.ejphar.2008.10.046.